Preparation and Characterization of ZnO Clusters inside Mesoporous Silica

Wen-Hua Zhang, Jian-Lin Shi,* Lian-Zhou Wang, and Dong-Sheng Yan

State Key Lab of High Performance Ceramics and Superfine Microstructure, Shanghai Institute of Ceramics, Chinese Academy of Sciences, Shanghai, 200050, China

Received November 24, 1999. Revised Manuscript Received January 26, 2000

Wide band-gap semiconductor−zinc oxide nanoclusters have been prepared in the channels of MCM-41 materials by functionalizing the MCM-41 with ethylenediamine groups, absorbing zinc cations, and calcinating at high temperatures. The products have been characterized by XRD, TEM, EDS, nitrogen adsorption and desorption, and UV−vis and PL spectroscopies. ZnO clusters were mostly confined and dispersed in the pores of mesoporous hosts. No large ZnO particles on the external surfaces have been detected. A massive blue-shift in UV−vis absorption spectra has been observed and large band increase can be expected. The nature of the PL spectrum has been attributed to the defects related to oxygen vacancies. In addition, the assembly of cobalt, nickel, and copper oxides inside MCM-41 materials has also been tried by this scheme, but at the moment, only the cobalt oxide can be prepared with good results. Unfortunately, noble metals have usually grown into large particles on the outside surface of MCM-41 by this scheme, e.g., a lot of silver particles with sizes much larger than the pore diameter of MCM-41 host have been obtained. However, the explanation is not yet clear.

Introduction

Since the discovery of the M41S family of mesoporous materials,[1,2] a new era in inclusion chemistry has began.[3] MCM-41, one member of the M41S family, possesses regularly hexagonal arrays of mesopores, changeable pore diameter between 1.5−30 nm and tailorable interior surfaces. These properties make MCM-41 materials among the best candidates as hosts for many guest materials. While the larger size of the pores is a prerequisite for many applications, it is by itself often not sufficient when specific surface properties are desired. Fortunately, specific surface properties can be introduced through proper surface modifications[4] and isomorphous substitution of Si by a tri- or tetravalent metal cation.[5] This discovery has stimulated research on the inclusion chemistry of mesoporous silica, including ion exchange,[5a,6] the assembly of metal,[7] metal oxide,[8] metal complex,[9] organometal,[10] and fullerenes.[11] Making use of the reactivity of the Si−OH groups on the internal pore surfaces of mesoporous silica, two main schemes have been developed to tailor the internal pore walls. One is by covalent grafting of ligands, including metal complexes,[9] organometallic compounds,[10] and chlorides.[12] These compounds all contain labile ligands that can be attached to the interior surface via direct reaction with Si−OH groups; another is by grafting silane coupling agents. For examples, solid acids,[13] bases,[14] and absorbent for metal ions[15] have been designed with this scheme.

* Corresponding author. E-mail: jlshi@sunm.shcnc.ac.cn. Fax: 86−21−62513903.

(1) Kresge, C. T.; Leonowicz, M. E.; Roth, W. J.; Vartuli, J. C.; Beck, J. S. *Nature* **1992**, *359*, 710.

(2) Beck, J. S.; Vartuli, J. C.; Roth, W. J.; Leonowicz, M. E.; Kresge, C. T.; Schmitt, K. D.; Chu, C. T.-W.; Olson, D. H.; Sheppard, E. W.; McCullen, S. B.; Higgins, J. B.; Schlenker, J. L. *J. Am. Chem. Soc.* **1992**, *114*, 10834.

(3) Moller, K.; Bein, T. *Chem. Mater.* **1998**, *10*, 2950 and references therein.

(4) For example, see: (a) Jaroniec, C. P.; Kruk, M.; Jaronic, M.; Sayari, A. *J. Phys. Chem.* B **1998**, *102*, 5503. (b) Koyano, K. A.; Tatsumi, T.; Tanaka, Y.; Nakzta, S. *J. Phys. Chem. B* **1997**, *101*, 9436.

(5) For example, see: (a) Kim, J. M.; Kwak, J. H.; Jun, S.; Ryoo, R. *J. Phys. Chem.* **1995**, *99*, 16742. (b) Zhang, W.; Fröba, M.; Wang, J.; Tanev, P. T.; Wong, J.; Pinnavaia, T. J. *J. Am. Chem. Soc.* **1996**, *118*, 9161. (c) Alba, M. D.; Luan, Z.; Klinowski, J. *J. Phys. Chem.* **1996**, *100*, 2178.

(6) Hartmann, M.; Pöppl, A.; Kevan, L. *J. Phys. Chem.* **1995**, *99*, 9.

(7) (a) Corma, A.; Martinez, A.; Martinez-Soria, V. J. *J. Catal.* **1997**, *169*, 480. (b) Koh, C. A.; Nooney, R.; Tahir, S. *Catal. Lett.* **1997**, *47*, 199.

(8) (a) Morey, M.; Davidson, A.; Eckert, H.; Stucky, D. *Chem. Mater.* **1996**, *8*, 486. (b) Kloetstra, K. R.; Van Laren, M.; Van Beckkum, H. *J. Chem. Soc. Faraday Trans.* **1997**, *93*, 1211.

(9) (a) Badiei, A.-B.; Bonneviot, L. *Inorganic Chem.* **1998**, *37*, 4142. (b) Weckhuysen, B. M.; Schoonheydt, R. A. *Chem. Commun.* **1999**, 445.

(10) (a) Maschmeyer, T.; Rey, F.; Sankar, G.; Thomas, J. M. *Nature* **1995**, *378*, 159. (b) Van Looveren, L. K.; Geysen, D. F.; Vercruysse, K A.; Wouters, B. H.; Grobet, P. J.; Jacobs, P. A. *Angew. Chem., Int. Ed. Engl.* **1998**, *37*, 517. (c) Zhou, W.; Thomas, J. M.; Shephard, D. S.; Johnson, B. F. G.; Ozkaya, D.; Maschmeyer, T.; Bell, R. G.; Ge, Q. *Science* **1998**, *280*, 705. (d) Shephard, D. S.; Maschmeyer, T.; Johnson, B. F. G.; Thomas, J. M.; Sankar, G.; Ozkaya, D.; Zhou, W.; Oldroyd, R. D.; Bell, R. G. *Angew. Chem., Int. Ed. Engl.* **1997**, *36*, 2242.

(11) (a) Gu, G.; Ding, W.; Du, Y.; Huang, Y.; Yang, S. *Appl. Phys. Lett.* **1997**, *70*, 2619. (b) Chen, J.; Li, Q.; Ding, H.; Pang, W.; Xu, R. *Langmuir* **1997**, *13*, 2050.

(12) (a) Ryoo. R.; Jun, S.; Kim, J. M.; Kim, M. J. *Chem. Commun.* **1997**, 2225. (b) Mokaya, R.; Jones, W. *J. Mater. Chem.* **1999**, *9*, 555.

(13) (a)Van Rhijin, W. M.; De Vos, D. E.; Sels, B. F.; Bossaert, W. D.; Jacobs, P. A. *Chem. Commun.* **1998**, 317. (b) Lim. M. H.; Blanford, C. F.; Stein, A. *Chem. Mater.* **1998**, *10*, 467.

(14) (a) Rao, Y. V. S.; De vos, D. E.; Jacobs, P. A. *Angew. Chem., Int. Ed. Engl.* **1997**, *36*, 2661. (b) Sutra, P.; Brunel, D. *Chem. Commun.* **1996**, 2485.

(15) (a) Feng, X.; Fryxell, G. E.; Wang, L.-Q.; Kim, A. Y.; Liu, J.; Kemner, K. M. *Science* **1997**, *276*, 923. (b) Mercier, L.; Pinnavaia, T. J. *Adv. Mater.* **1997**, *9*, 500. (c) Diaz, J. F.; Balkus, K, J., Jr.; Bedioui, F.; Kurshev, V.; Kevan, L. *Chem. Mater.* **1997**, *9*, 61.

10.1021/cm990740a CCC: $19.00
Published on Web 04/06/2000

Mesoporous solids loaded with nanoscaled particles within their pores have received considerable attention in recent years, especially semiconductor nanoparticles, which may have found great applications in optoelectronic devices. Fe_2O_3 nanoparticles have been introduced into the pores of MCM-41 by the incipient wetness method.[16] Ge QWRs[17] inside the channels of MCM-41 have been fabricated by thermal treatment of Ge_2H_6 absorbed in MCM-41. TiO_2[18] has been grafted onto the frameworks of MCM-41 by reacting $TiCl_4$ with the parent mesostructured silicate. GaAs[19] and InP[20] have been deposited into the channels of MCM-41 by MOCVD methods. CdS nanoclusters[21] absorbed into channels of MCM-41 functionalized by thiol groups and silicon clusters[22] formed in the mesoporous silica film have also been reported. All of these semiconductor nanoparticles inside MCM-41 show the size quantization effects. Additionally, In_2O_3 nanoprticles have also been prepared in the irregular mesoporous silica,[23] and novel photoluminescence properties have been observed.

ZnO is a wide band-gap semiconductor and is of great interest for short wavelength electrooptic devices. The nanocrystalline thin films of ZnO have been prepared by variable methods, such as microwave plasma-enhanced molecular beam epitaxy (MBE),[24] laser enhanced MBE,[25] radical beam epitaxy,[26] and electrophetic deposition methods.[27] The preparation of quantum size ZnO particles has been obtained through sol−gel methods by several groups in recent years.[28] In this paper, we report a new scheme to synthesize ZnO nanoparticles by using mesoporous silica MCM-41 as host materials. By functionalizing mesoporous silica MCM-41 with ethylenediamine groups (ED-MCM-41), and using it as absorbent for Zn^{2+} (Zn-ED-MCM-41), ZnO nanoparticles would be obtained after the Zn-ED-MCM-41 was calcinated in air. The products were extensively characterized by powder X-ray diffraction (XRD), transmission electron microscopy (TEM), energy dispersive spectra (EDS), N_2 adsorption−desorption isotherms, UV−vis diffuse reflectance spectra and photoluminescence (PL) spectra. Experiments show that the ZnO particles are mostly confined in the pores of MCM-41 and size quantization effects have been observed. Because of the fact that the high surface area of MCM-41 materials is attributed to the particular pore system, and the major fraction of free surface is at the inside of the pores, the functionalizing reaction should mainly occur in the internal surfaces of MCM-41. Therefore, the ZnO clusters prepared in this scheme should be essentially confined in the pores and the amount of ZnO clusters on the external surfaces should be much less than that in the channels. In addition, other metal oxides, such as cobalt, nickel, and copper oxides, can also be prepared by this scheme, but only the cobalt oxides can be prepared with good results. However, noble metal or metal oxides have been shown to grow into large particles on the outside surface of mesoporous materials by this scheme.

Experimental Section

Pure siliceous MCM-41 samples were prepared by the hydrolysis of cetyl- trimethyamonium bromide (CTAB) and tetraethyl silicate (TEOS) in basic solution, the final composition is 1.0 CTAB:7.5 TEOS:1.8 NaOH:500 H_2O (molar ratio), then hydrothermally treated at 110 °C for 60 h. Functional groups (ethylenediamine groups in this case) were introduced to the pore surfaces of mesoporous silica by refluxing the mixture of the calcined MCM-41 and *N*-[3-(trimethoxysilyl)-propylethylene]diamine (designated as TPED) (1 g of MCM-41 to 5 mL of TPED) in dry toluene under nitrogen atmosphere for at least 10 h. The resulting hybrid materials (ED-MCM-41) are efficient absorbers for metal ions of IB, IIB, and VIII groups in water and ethanol solutions because ethylenediamine groups have a strong ability to complex these ions. To avoid the hydrolysis or even collapses of the siliceous frameworks in water, Zn^{2+} was absorbed into the ED-MCM-41 by soaking and stirring the ED-MCM-41 in 0.002, 0.01, and 0.05 M $Zn(CH_3COO)\cdot 2H_2O$/ethanol solutions, and Zn-ED-MCM-41 samples resulted after being filtered and washed with ethanol. These Zn containing samples are designated as Zn-ED-MCM-41(0.002), -(0.01), and -(0.05), respectively. Similar designations are also used in later sections. To remove the small amount of Zn^{2+} in the channels and on the outside surfaces of MCM-41 but are not complexed by ethylenediamine groups, these Zn-ED-MCM-41 samples were soaked and stirred in ethanol, filtered, and washed with ethanol, and this process was repeated three times. The resulting samples can be used for later treatments. Finally, the Zn-ED-MCM-41 samples were calcinated at 600 °C in air for 10 h to remove the organic components. Thus, ZnO-MCM-41 composites were obtained.

The powder XRD patterns were recorded with Rigaku Rotaflex diffractometer equipped with a rotating anode and using Cu Kα radiation over the range of $1.8° \leq 2\theta \leq 70°$. Si was used as the internal standard. TEM and EDS analyses were performed using a JEOL 200CX electron microscope operating at 200 kV. The N_2 adsorption−desorption isotherms were obtained on a Micromeritics TriStar 3000 at 77 K under continuous adsorption condition. BET and BJH analyses were used to determine the total specific surface area (S_{BET}) and the pore size distribution. UV−vis diffusing reflectance spectra were measured on a Shimadzu UV-3101 equipped with an integrating sphere using $BaSO_4$ as the reference. Photoluminescence (PL) spectra were recorded on a Shimadzu RF-5301 PC spectrofluorophotometer at room temperature. Wet chemical analysis was used to determine the zinc content.

Results and Discussion

Powder X-ray diffraction (XRD) patterns for the series of MCM-41 samples are shown in Figure 1. All of the as-synthesized samples display three reflection peaks, which are characteristic of MCM-41 materials. Therefore, the hexagonal ordered structure was maintained

(16) Abe, C.; Tachibana, Y.; Uematsu, T.; Iwamoto, M. *Chem. Commun.* **1995**, 1617.
(17) Leon, R.; Margolese, D.; Stucky, G. D.; Petroff, P. M. *Phys. Rev. B:* **1995**, 52, 2285.
(18) Aronson, B. J.; Blanford, C.; Stein, A. *Chem. Mater.* **1997**, 9, 2842.
(19) Srdanov, V. I.; Alxneit, I.; Stucky, G. D.; Reaves, C. M.; DenBaars, S. P. J. Phys. Chem. B. **1998**, *102*, 3341.
(20) Agger, J. R.; Anderson, M. W.; Pemble, M. E.; Terasaki, O.; Nozue, Y. *J. Phys. Chem. B* **1998**, 102, 2345.
(21) Hirai, T.; Okubo, H.; I. Komasawa, I. *J. Phys. Chem. B* **1999**, 103, 4228.
(22) Dag, Ö.; Ozin, G. A.; Yang, H.; Reber, C.; Bussiere, G. *Adv. Mater.* **1999**, *11*, 474.
(23) Zhou, H.; Cai, W.; Zhang, L. *Mater. Res. Bull.* **1999**, *34*, 845.
(24) Bagnall, D. M.; Chen, Y. F.; Zhu, Z.; Yao, T.; Koyama, S.; Shen, M. Y.; Goto, T. *Appl. Phys. Lett.* **1997**, *70*, 2230.
(25) Ohtomo, A.; Kawasaki, M.; Sakurai, Y.: Yoshida, Y.; Koinuma, H.; Yu, P.; Kang, Z. K.; Wong, G. K. L.; Segawa, Y. *Mater Sci. Eng. B* **1998**, *54*, 24.
(26) Bulkhuzi, T. V.; Chelidze, T. G.; Georgobiani, A. N.; Jashiashvili, T. G.; Tsekvava, B. E. *Phys. Rev. B* **1998**, *58*, 10692.
(27) Wong, E. M.; Searson, P. C. *Appl. Phys. Lett.* **1999**, *74*, 2939.
(28) (a) Bahnemann, D. W.; Kormann, C.; Hoffmann, M. R. *J. Phys. Chem.* **1987**, *91*, 3789. (b) Haase, M.; Weller, H.; Henglein, A. *J. Phys. Chem.* **1988**, *92*, 482. (c) Spanhel, L.; Anderson, M. A. *J. Am. Chem. Soc.* **1991**, *113*, 2826. (d) Kamat, P. V.; Patrick, B. *J. Phys. Chem.* **1992**, *96*, 6829.

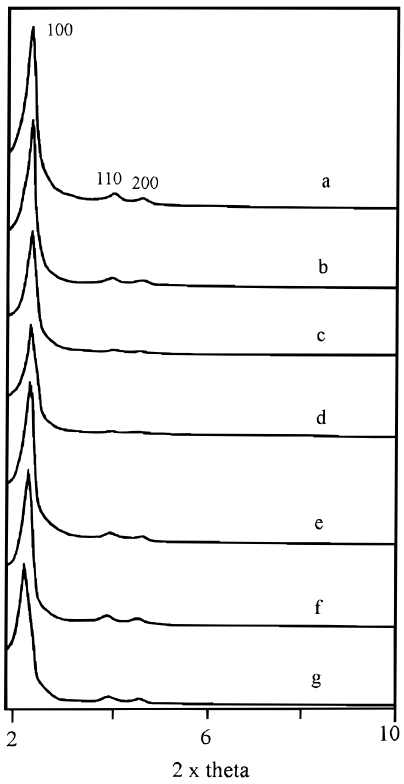

Figure 1. XRD patterns of series of MCM-41: (a) calcined MCM-41, (b) calcined ED-MCM-41, (c) ED-MCM-41, (d) Zn-ED-MCM-41(0.05), (e) ZnO-MCM-41(0.002), (f) ZnO-MCM-41-(0.01), and (g) ZnO-MCM-41(0.05).

during the formation process of ZnO clusters. The ED-MCM-41 and Zn-ED-MCM-41 samples demonstrated a marked loss of peak intensity for the low-angle reflections. However, the removal of the organic component by calcinating at higher temperature recovers the peak intensity to a certain degree. On the other hand, the peak loss also increases with the increase of the ZnO content for ZnO-MCM-41 samples; therefore, the decrease of peak intensity should be attributed to both organic component and ZnO clusters. Organic sorbates inside MCM-41 also have similar effects on the XRD patterns.[29] Compared to the calcinated MCM-41 sample, all peaks shift slightly to higher angles for ZnO-containing samples. This is probably due to the contraction of the frameworks which may arise from the high-temperature calcination. The XRD patterns for all of these samples within the range of 10−70° show only the diffuse peaks of noncrystalline silica frameworks, and no characteristic peaks belonging to the ZnO have been observed. This shows that ZnO clusters may be fully dispersed inside MCM-41. The formation of ZnO inside MCM-41 seems to strengthen the frameworks of MCM-41. For comparison purposes, the ED-MCM-41 sample was calcinated at conditions identical to Zn-ED-MCM-41 samples (this calcinated ED-MCM-41 is designated as ED-MCM-41 (cal)) and was found to contract more than that of ZnO containing samples. The degree of contraction decreases with the increase of ZnO content, as shown in Table 1. This suggests that ZnO clusters can prevent the contraction of the frameworks

(29) Marler, B.; Oberhagemann, U.; Vortamann, S.; Gies, H. *Microporous Mater.* **1996**, *6*, 375.

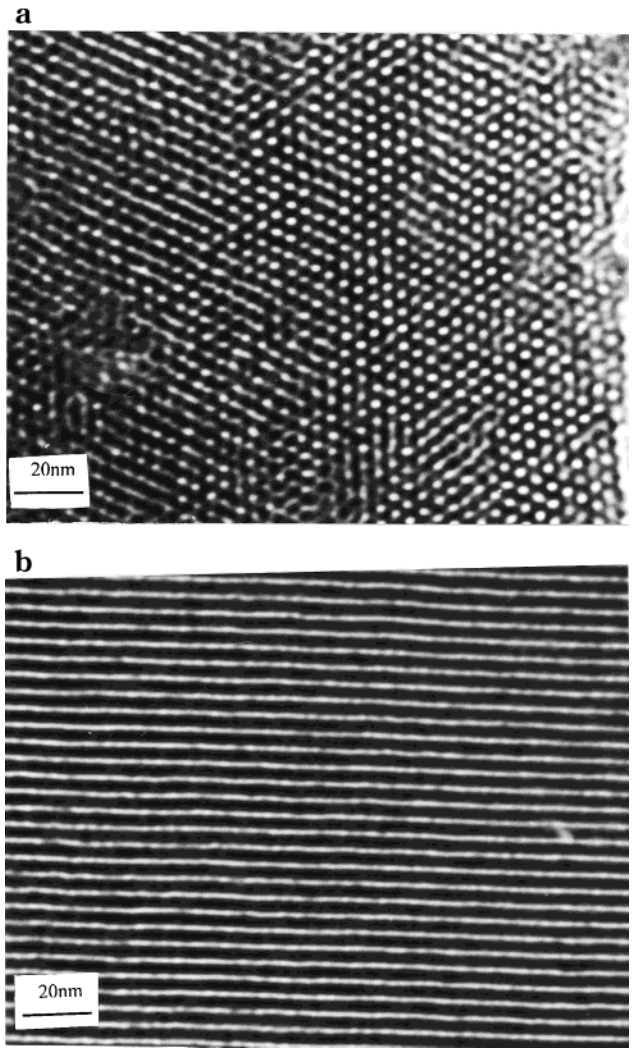

Figure 2. HRTEM images of ZnO-MCM-41(0.05) sample: (a) the micrograph taken with the beam direction parallel to the pore and (b) the micrograph taken with the beam direction perpendicular to the pore.

Table 1. Parameters of the Series of the As-Prepared MCM-41 Samples

sample	ZnO content (wt%)	d_{100} (Å)	surface area (m^2/g)	pore diameter (Å)	pore volume (cm^3/g)
MCM-41		38.9	1027	26.8	0.52
ED-MCM-41(cal)		38.3	884	26.2	0.41
ZnO-MCM-41(0.002)	1.08	38.3	820	25.5	0.38
ZnO-MCM-41(0.01)	3.99	38.4	791	25.5	0.35
ZnO-MCM-41(0.05)	9.34	38.5	734	25.3	0.30

of mesoporous silica upon calcination. A similar result has been reported in the TiO_2-MCM-41 system.[18] However, contrary effects have also been reported in the V_2O_5-MCM-48 [30] and Fe_2O_3 -MCM-41 [16] systems.

Further evidence that the highly ordered pore structure has been preserved during the formation process of ZnO clusters inside MCM-41 is provided by transmission electron micrographs, as shown in Figure 2. In the micrographs taken with the beam direction parallel to the pore direction (Figure 2a), the hexagonally ordered pore structure can clearly be observed, and no image of ZnO particles have been found on the outside surfaces. On the other hand, the micrographs taken with the beam direction perpendicular to the pores (Figure 2b)

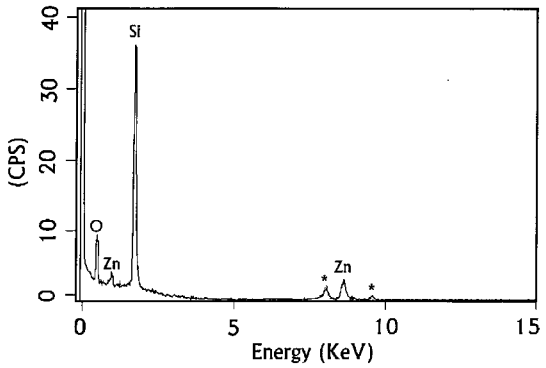

Figure 3. EDS spectrum of the ZnO-MCM-41 (abs) sample (*) is Cu element which arises from the support grid.

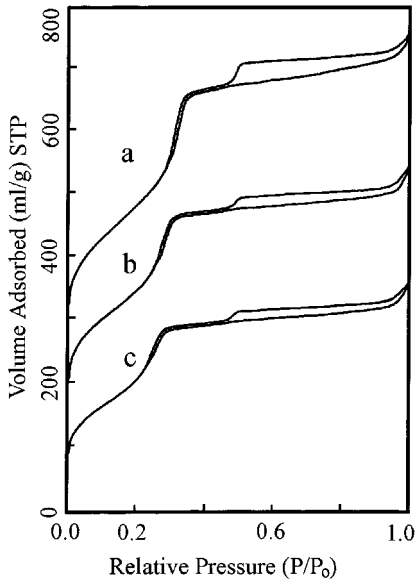

Figure 4. Nitrogen adsorption−desorption isotherms of series of MCM-41 samples: (a) calcined MCM-41, (b) calcined ED-MCM-41, and (c) ZnO-MCM-41(0.05).

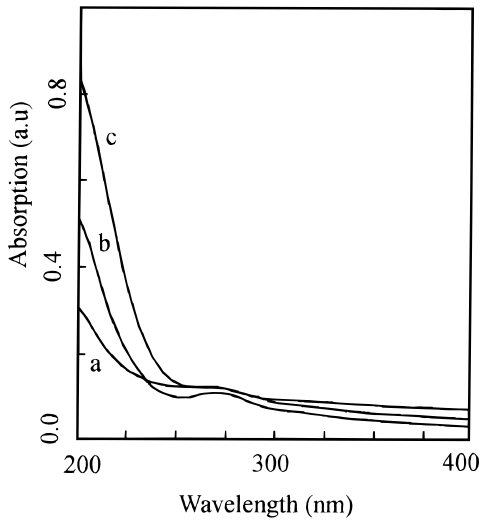

Figure 5. Diffuse-reflectance UV−vis spectra of ZnO containing samples: (a) ZnO-MCM-41(0.002), (b) ZnO-MCM-41(0.01), and (c) ZnO-MCM-41(0.05).

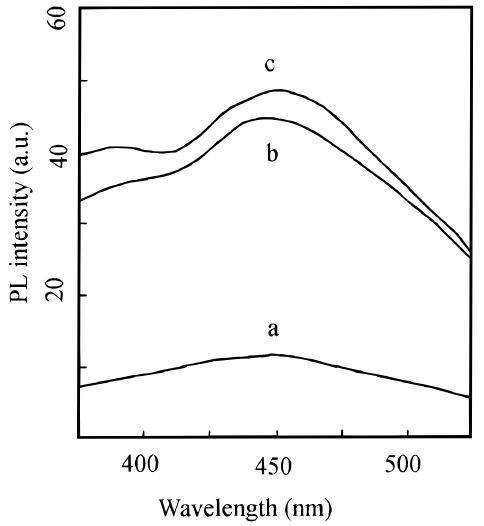

Figure 6. PL spectra of ZnO containing samples: (a) ZnO-MCM-41(0.002), (b) ZnO-MCM-41(0.01), and (c) ZnO-MCM-41(0.05). The PL spectra were all taken at room temperature.

only showed the images of channels and frameworks of MCM-41 materials. The images of ZnO clusters on the outside surface of MCM-41 have still not been found. However, the functional groups can be bonded to both the external and internal surfaces of MCM-41, so some ZnO clusters should also exist on the outside surfaces. It is well-known that the high surface area of MCM-41 materials is mainly attributed to the pore system and a relatively small part to the external surfaces, so the functionalizing reaction should mainly occur at the internal surfaces of MCM-41. Therefore, the ZnO clusters prepared by this scheme should be mostly confined in the pores and the amount of ZnO clusters on the external surfaces should be much less than that in the channels. We have attempted, but failed to directly observe the particles of ZnO in the channels of MCM-41 by TEM method. This is probably due to the fact that the contrast between the silica frameworks of MCM-41 and ZnO clusters is too weak, as the case of Fe_2O_3 inside mesoporous host.[16] To confirm the presence of ZnO in the channels of MCM-41, EDS (Figure 3) analysis on these areas was carried out and produced strong zinc signals. EDS measurement also shows that ZnO is present in all areas of MCM-41, but the distribution is not very homogeneous. The content of ZnO near to the opening of the pores is slightly higher than that in the inner part of the pores. The possible reason is that the part of the pore near to the opening can fully contact with the organosilanes, and more ethylenediamine groups can be anchored onto these areas than that in the inner part of the pores. Chemical analysis shows the ZnO content is 1.02, 3.99, and 9.04 wt % for ZnO-MCM-41(0.002), -(0.01), and -(0.05) samples, respectively. These data are all smaller than the corresponding data given by EDS methods.

Nitrogen adsorption and desorption properties provide the information on the pore characteristics of these systems. The parameters calculated from these data for the as-prepared series of MCM-41 samples are listed in the Table 1. The decrease of BET surface areas, average pore diameters and pore volumes with the increase of ZnO content indicates that ZnO clusters should be confined in the pores of MCM-41. The isotherms are all type IV classification (Figure 4), which is characteristic of adsorption of mesoporous materials. A sharp increase in the adsorption amount of nitrogen

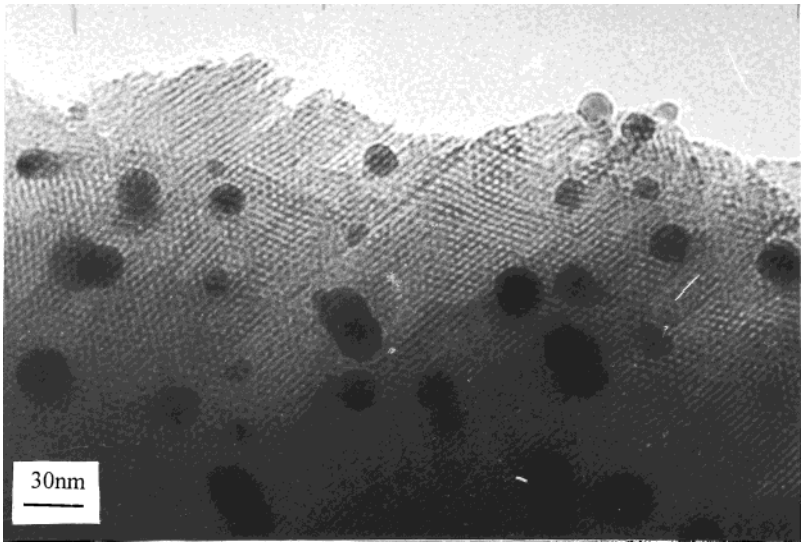

Figure 7. HRTEM image of Ag-MCM-41 sample.

at the relative pressure of $P/P_0 > 0.25$ can be seen for all the samples, which is due to capillary condensation. Combination of hysteresis of type H1 and H4 can be observed on all samples. Type H1 hysteresis, whose loop appears on the vertical portion of type IV isotherm, is usually produced for mesoporous materials with cylindrical pores. The type H4 hysteresis, in which the loop is seen on the horizontal portion, is believed to represent slit-shaped pores with some microporosity. Detailed analysis of H4 hysteresis in MCM-41 materials has been reported in reference.[18] The isotherms for the Zn containing samples were similar in shape to the parent MCM-41 sample, which suggests that the ZnO clusters should be dispersed throughout the pores. The mesoporous channels are still accessible even after the formation of ZnO clusters inside MCM-41. The type of H2 hysteresis is commonly associated with ink bottle shaped pores, in which the area near the opening is narrower than the main body of the pore. Although the ZnO content near the opening of the pores is slightly higher than that in the interior part, a type H2 hysteresis loop has not been observed. Therefore, ZnO nanoparticles should not be only concentrated on the openings, but dispersed over the pore channels.

The UV−vis diffusing reflectance spectra for as-prepared ZnO-MCM-41 samples are shown in Figure 5. The pure siliceous MCM-41 gives very little absorption in this range.[16] The onsets of absorption of the as-prepared ZnO containing samples are all near to 290 nm. However, macrocrystalline ZnO starts to absorb close to 370 nm.[28a] This massive blue-shift in the absorption spectra reflects an increasing band gap of the semiconductor which arises from the size quantization effect. By comparing the present results to the λ_{onset} versus 2R relationship of ZnO colloids reported by Haase et al.,[28b] the diameter of the as-prepared ZnO clusters is estimated to be less than 1.8 nm, which is smaller than the pore diameter of the ED-MCM-41 (cal) host (~2.62 nm) and consistent with the inference that ZnO clusters should be located in the channels of MCM-41. Taking the above results into consideration, including XRD patterns, TEM, EDS, nitrogen adsorption−desorption isotherms, and UV−vis spectra analysis, ZnO clusters should mainly be formed and retained in the channels, and may only be small a part on the external surfaces of the MCM-41 hosts. The ZnO clusters may have formed monolayers loosely attached onto the internal surfaces of MCM-41 materials.

Room-temperature PL spectra of the as-synthesized ZnO containing samples are shown in Figure 6. The PL peaks are all near 450 nm and their intensities increase with the ZnO content; a similar case also occurred in the UV−vis spectra. The emission of the as-prepared ZnO-containing samples is Stokes-shifted from the absorption spectra, which arises from midgap states. So the PL emission should be attributed to defect luminescence. The nature of the visible fluorescence is controversial.[28] Crystalline ZnO is a self-activated phosphor with a band gap of 3.1 eV. The green luminescence of ZnO is characteristic of phophors fired in air or under reducing conditions (H_2, ZnS, CO, etc.) for bulk crystallines.[31] Excess Zn has been detected by a chemical analysis. Interstitial zinc and oxygen vacancies are considered to be the dominant defects. On the other hand, ZnO nanoparticles prepared in colloids have been shown to exhibit similar green emissions around 450−600 nm, which were believed to originate from anion vacancies.[28b] Similar results have also been reported by another group.[28d] Finally, Vanheusden et al.[32] have recently studied the mechanism of the photoluminescence of ZnO powders and attributed the green emission to the singly ionized oxygen vacancies. Very recently, Mao et al.[33] have reported that ZnO nanoparticles in the irregular mesoporous silica showed a dramatic enhancement effect of photoluminescence, which has also been believed to originate from the singly ionized oxygen vacancies. So the PL emission in the present experiments should very likely be attributed to defects related to oxygen vacancies. The massive shift to short wavelength in the PL peaks should arise from the size quantization effects, because the size of the ZnO clusters

(30) Morey, M.; davidson, A.; Eckert, H.; Stucky, G. D. *Chem. Mater.* **1996**, *8*, 486.
(31) Liu, M.; Kitai, A. H.; Mascher, P. *J. Lumin.* **1992**, *54*, 35.
(32) Vanheusden, K.; Warren, W. L.; Seager, C. H.; Tallant, D. R.; Voigt, J. A.; Gnade, B. E. *J. Appl. Phys.* **1996**, *79*, 7983.
(33) Mao, C. M.; Li, Y.; Liu, Y. S.; Zhang, Y.; Zhang, L. D. *J. Appl. Phys.* **1998**, *83*, 4389.

in the present experiment is much smaller than that reported by Mao.

Finally, we have also exploited the possibility to prepare other metal oxides inside MCM-41 by this scheme. Unexpectedly, only cobalt oxide can be prepared in the channels of MCM-41 with good results. Some nickel and copper oxides would be leached out after calcination at 600 °C to remove the organic component. These results are preliminary and can be improved by calcinating the samples at lower temperatures for a shorter period of time under oxygen atmosphere. More unfortunately, as to those noble cations that can be absorbed by ethylenediamine groups, such as Ag^{+}, $AuCl_4^{+}$, and Pd^{2+}, heat treatment at high temperature to remove the organic component induces the formation of large particles on the outside surface of MCM-41 by this scheme. Figure 7 shows the TEM micrograph of a Ag-containing sample prepared by the same process as that of ZnO-MCM-41. Particle sizes of silver up to 30 nm have been obtained. The explanation is not yet clear. High mobility at high temperatures for these metal ions could be a reason and further work should be carried out.

Conclusion

The present study demonstrates that ZnO nanoparticles can be prepared in the channels of MCM-41 by a surface modification scheme with multiple steps. Combined spectroscopic and bulk structural characterizations showed that ZnO clusters have been formed and dispersed mainly in the pores of mesoporous materials. The great blue-shifts in the absorption spectra and PL emission for ZnO containing samples are attributed to the size quantization effects. The PL centers are believed to be defects related with oxygen vacancies. In addition, cobalt oxide clusters can also be prepared inside MCM-41 by this scheme. However, those noble metals, such as silver, gold, and palladium, grow into large particles on the outside surface of MCM-41 materials prepared by this scheme and the explanation is not yet clear.

Acknowledgment. This work was supported by National Natural Science Foundation of China, grant 59882007.

CM990740A